INTERNATIONAL STANDARD

ISO 20998-2

Second edition
2022-08

# Measurement and characterization of particles by acoustic methods —

## Part 2:
## Linear theory

*Caractérisation des particules par des méthodes acoustiques —*

*Partie 2: Théorie linéaire*

Reference number
ISO 20998-2:2022(E)

ISO copyright office
CP 401 • Ch. de Blandonnet 8
CH-1214 Vernier, Geneva
Phone: +41 22 749 01 11
Email: copyright@iso.org
Website: www.iso.org

Published in Switzerland

# Contents

Page

**Foreword** .... **iv**

**Introduction** .... **v**

**1 Scope** .... **1**

**2 Normative references** .... **1**

**3 Terms and definitions** .... **1**

**4 Symbols and abbreviations** .... **2**

**5 Mechanism of attenuation (dilute case)** .... **4**
- 5.1 Introduction .... 4
- 5.2 Excess attenuation coefficient .... 4
- 5.3 Specific attenuation mechanisms .... 5
  - 5.3.1 Scattering .... 5
  - 5.3.2 Thermal losses .... 5
  - 5.3.3 Viscoinertial losses .... 5
  - 5.3.4 Non-monotonic relaxation mechanisms .... 5
- 5.4 Linear models .... 5
  - 5.4.1 Review .... 5
  - 5.4.2 Physical parameters .... 6

**6 Determination of particle size** .... **7**
- 6.1 Introduction .... 7
- 6.2 Inversion approaches used to determine PSD .... 8
  - 6.2.1 Optimization of a PSD function .... 8
  - 6.2.2 Regularization .... 8
- 6.3 Limits of application .... 9

**7 Instrument qualification** .... **9**
- 7.1 Calibration .... 9
- 7.2 Precision .... 9
  - 7.2.1 Reference samples .... 9
  - 7.2.2 Repeatability .... 10
  - 7.2.3 Reproducibility .... 10
- 7.3 Accuracy .... 10
  - 7.3.1 Qualification procedure .... 10
  - 7.3.2 Reference samples .... 10
  - 7.3.3 Instrument preparation .... 10
  - 7.3.4 Accuracy test .... 10
  - 7.3.5 Qualification acceptance criteria .... 10

**8 Reporting of results** .... **11**

**Annex A** (informative) **Viscoinertial loss model** .... **12**

**Annex B** (informative) **ECAH theory and limitations** .... **13**

**Annex C** (informative) **Example of a semi-empirical model** .... **17**

**Annex D** (informative) **Iterative fitting** .... **20**

**Annex E** (informative) **Physical parameter values for selected materials** .... **22**

**Annex F** (informative) **Practical example of PSD measurement** .... **23**

**Bibliography** .... **32**

# Foreword

ISO (the International Organization for Standardization) is a worldwide federation of national standards bodies (ISO member bodies). The work of preparing International Standards is normally carried out through ISO technical committees. Each member body interested in a subject for which a technical committee has been established has the right to be represented on that committee. International organizations, governmental and non-governmental, in liaison with ISO, also take part in the work. ISO collaborates closely with the International Electrotechnical Commission (IEC) on all matters of electrotechnical standardization.

The procedures used to develop this document and those intended for its further maintenance are described in the ISO/IEC Directives, Part 1. In particular, the different approval criteria needed for the different types of ISO documents should be noted. This document was drafted in accordance with the editorial rules of the ISO/IEC Directives, Part 2 (see www.iso.org/directives).

Attention is drawn to the possibility that some of the elements of this document may be the subject of patent rights. ISO shall not be held responsible for identifying any or all such patent rights. Details of any patent rights identified during the development of the document will be in the Introduction and/or on the ISO list of patent declarations received (see www.iso.org/patents).

Any trade name used in this document is information given for the convenience of users and does not constitute an endorsement.

For an explanation of the voluntary nature of standards, the meaning of ISO specific terms and expressions related to conformity assessment, as well as information about ISO's adherence to the World Trade Organization (WTO) principles in the Technical Barriers to Trade (TBT), see www.iso.org/iso/foreword.html.

This document was prepared by Technical Committee ISO/TC 24, *Particle characterization including sieving*, Subcommittee SC 4, *Particle characterization*.

This second edition cancels and replaces the first edition (ISO 20998-2:2013), which has been technically revised.

The main changes are as follows:

- References to relaxation mechanisms that affect attenuation
- Additional explanatory notes for Table 1
- Clarification of notation used in Formula (9)
- Minor editorial changes

A list of all parts in the ISO 20998 series can be found on the ISO website.

Any feedback or questions on this document should be directed to the user's national standards body. A complete listing of these bodies can be found at www.iso.org/members.html.

# Introduction

It is well known that ultrasonic spectroscopy can be used to measure particle size distribution (PSD) in colloids, dispersions, and emulsions[1],[2],[3],[4]. The basic concept is to measure the frequency-dependent attenuation or velocity of the ultrasound as it passes through the sample. The attenuation spectrum is affected by scattering or absorption of ultrasound by particles in the sample, and it is a function of the size distribution and concentration of particles[5],[6],[7]. Once this relationship is established by empirical observation or by theoretical calculations, one can estimate the PSD from the ultrasonic data. Ultrasonic techniques are useful for dynamic online measurements in concentrated slurries and emulsions.

Traditionally, such measurements have been made off-line in a quality control lab, and constraints imposed by the instrumentation have required the use of diluted samples. By making in-process ultrasonic measurements at full concentration, one does not risk altering the dispersion state of the sample. In addition, dynamic processes (such as flocculation, dispersion, and comminution) can be observed directly in real time[8]. This data can be used in process control schemes to improve both the manufacturing process and the product performance.

While it is possible to determine the particle size distribution from either the attenuation spectrum or phase velocity spectrum, the use of attenuation data alone is recommended. The relative variation in phase velocity due to changing particle size is small compared to the mean velocity, so it is often difficult to determine the phase velocity with a high degree of accuracy, particularly at ambient temperature. Likewise, the combined use of attenuation and velocity spectra to determine the particle size is not recommended. The presence of measurement errors (i.e. "noise") in the magnitude and phase spectra can increase the ill-posed nature of the problem and reduce the stability of the inversion.

# Measurement and characterization of particles by acoustic methods —

## Part 2:
## Linear theory

## 1 Scope

This document specifies requirements for ultrasonic attenuation spectroscopy methods for determining the size distributions of a particulate phase dispersed in a liquid at dilute concentrations, where the ultrasonic attenuation spectrum is a linear function of the particle volume fraction. In this regime particle-particle interactions are negligible. Colloids, dilute dispersions, and emulsions are within the scope of this document. The typical particle size for such analysis ranges from 10 nm to 3 mm, although particles outside this range have also been successfully measured. For solid particles in suspension, size measurements can be made at concentrations typically ranging from 0,1 % by volume up to 5 % by volume, depending on the density contrast between the solid and liquid phases, the particle size, and the frequency range[9],[10]. For emulsions, measurements can be made at much higher concentrations. These ultrasonic methods can be used to monitor dynamic changes in the size distribution.

## 2 Normative references

The following documents are referred to in the text in such a way that some or all of their content constitutes requirements of this document. For dated references, only the edition cited applies. For undated references, the latest edition of the referenced document (including any amendments) applies.

ISO 14488, *Particulate materials — Sampling and sample splitting for the determination of particulate properties*

ISO 20998-1:2006, *Measurement and characterization of particles by acoustic methods — Part 1: Concepts and procedures in ultrasonic attenuation spectroscopy*

## 3 Terms and definitions

For the purposes of this document, the terms and definitions given in ISO 20998-1 and the following apply.

ISO and IEC maintain terminology databases for use in standardization at the following addresses:

— ISO Online browsing platform: available at https://www.iso.org/obp

— IEC Electropedia: available at https://www.electropedia.org/

**3.1**
**coefficient of variation**
ratio of the standard deviation to the mean value

**3.2**
**dimensionless size parameter**
representation of particle size as the product of *wavenumber* (3.4) and *particle radius* (3.3)

**3.3**
**particle radius**
half of the particle diameter

**3.4**

**wavenumber**

ratio of 2π to the wavelength

## 4 Symbols and abbreviations

For the purposes of this document, the following abbreviations and symbols apply.

| | |
|---|---|
| $\boldsymbol{A}$ | matrix representing the linear attenuation model |
| $A_n$ | coefficients of series expansion in ECAH theory |
| $a$ | particle radius |
| $c$ | speed of sound in liquid |
| $C_\mathrm{p}$ | specific heat at constant pressure |
| $C_\mathrm{PF}$ | particle projection area divided by suspension volume |
| CV | coefficient of variation (ratio of the standard deviation to the mean value) |
| $E$ | extinction at a given frequency |
| ECAH | Epstein-Carhart-Allegra-Hawley (theory) |
| $f_i$ | frequency |
| $g()$ | an arbitrary function |
| $\boldsymbol{H}$ | identity matrix |
| $h_\mathrm{n}$ | Hankel functions of the first kind |
| $I$ | transmitted intensity of ultrasound |
| $I_0$ | incident intensity of ultrasound |
| $i$ | the imaginary number |
| **inv()** | matrix inverse operation |
| $K$ | extinction efficiency (extinction cross-section divided by particle projection area) |
| $\boldsymbol{K}$ | matrix representation of the kernel function (the ultrasonic model) |
| $\boldsymbol{K}^\mathrm{T}$ | transpose of matrix $\boldsymbol{K}$ |
| $k(f, x)$ | kernel function |
| $k_\mathrm{c}$, $k_\mathrm{T}$, $k_\mathrm{s}$ | wave numbers of the compressional, thermal, and shear waves |
| $k.a$ | dimensionless size parameter |
| $ln()$ | natural logarithm |
| $P_n$ | Legendre polynomials |
| PSD | particle size distribution |
| $\boldsymbol{q}$ | solution vector (representation of the PSD) |

| | |
|---|---|
| $q_3(x)$ | volume weighted density function of the PSD |
| $Q_3(x)$ | volume weighted cumulative PSD |
| $s$ | standard deviation |
| $x$ | particle diameter |
| $x_{10}$ | the 10th percentile of the cumulative PSD |
| $x_{50}$ | median size (50th percentile) |
| $x_{90}$ | the 90th percentile of the cumulative PSD |
| $\mathrm{x}_{\mathrm{min}}$, $\mathrm{x}_{\mathrm{max}}$ | minimum and maximum particle diameters in a sample |
| $\alpha$ | total ultrasonic attenuation coefficient |
| $\boldsymbol{\alpha}$ | attenuation spectrum |
| $\tilde{\alpha}$ | absolute attenuation coefficient divided by the frequency, $\tilde{\alpha} = (\alpha / f)$ |
| $\alpha_{\mathrm{exc}}$ | excess attenuation coefficient, $\alpha_{exc} = \alpha - \alpha_L$ |
| $\alpha_{\mathrm{exc'}}$ | alternate definition of excess attenuation coefficient where $\alpha_{exc'} = \alpha - \alpha_{\mathrm{int}}$ |
| $\alpha_{\mathrm{exp}}$ | measured attenuation spectrum |
| $\alpha_{\mathrm{int}}$ | intrinsic absorption coefficient of the dispersion |
| $\alpha_{\mathrm{L}}$ | attenuation coefficient of the continuous (liquid) phase |
| $\alpha_{\mathrm{mod}}$ | attenuation spectrum predicted by the model, given a trial PSD |
| $\alpha_{\mathrm{P}}$ | attenuation coefficient of the discontinuous (particulate) phase |
| $\alpha_{\mathrm{sc}}$ | elastic scattering component of the attenuation coefficient |
| $\alpha_{\mathrm{th}}$ | thermal loss component of the attenuation coefficient |
| $\alpha_{\mathrm{vis}}$ | viscoinertial loss component of the attenuation coefficient |
| $\beta_{\mathrm{T}}$ | volume thermal expansion coefficient |
| $\mathit{\Delta}$ | error in the fit |
| $\delta$ | Tikhonov regularization factor |
| $\Delta l$ | thickness of the suspension layer |
| $\Delta Q_2$ | fraction of the total projection area containing a certain particle size class |
| $\eta$ | viscosity of the liquid |
| $\kappa$ | thermal conductivity |
| $\lambda$ | ultrasonic wavelength |
| $\mu$ | shear modulus |
| $\rho$, $\rho'$ | density of the liquid and particle, respectively |

| | |
|---|---|
| $\phi$ | volume concentration of the dispersed phase |
| $\chi^2$ | Chi-squared value |
| $\psi_c$ | compression wave |
| $\psi_s$ | shear wave |
| $\psi_T$ | thermal wave |
| $\omega$ | angular frequency (i.e. 2π times the frequency) |

## 5 Mechanism of attenuation (dilute case)

### 5.1 Introduction

As ultrasound passes through a suspension, colloid, or emulsion, it is scattered and absorbed by the discrete phase with the result that the intensity of the transmitted sound is diminished. The attenuation coefficient is a function of ultrasonic frequency and depends on the composition and physical state of the particulate system. The measurement of the attenuation spectrum is described in ISO 20998-1.

### 5.2 Excess attenuation coefficient

The total ultrasonic attenuation coefficient $\alpha$ is given by the viscoinertial loss, thermal loss, elastic scattering, and the intrinsic absorption coefficient $\alpha_{\text{int}}$ of the dispersion[1],[10] which can also include a variety of relaxation effects not alluded to in Reference [1] and [10], for example, solvent-ion and macromolecule-solvent effects which need to be accounted for separately due to their differing non-monotonic frequency dependencies[11],[12],[13].

$$\alpha = \alpha_{\text{vis}} + \alpha_{\text{th}} + \alpha_{\text{sc}} + \alpha_{\text{int}} \tag{1}$$

The intrinsic absorption is determined by the absorption of sound in each homogenous phase of the dispersion. For pure phases the absorption coefficients, denoted $\alpha_L$ for the continuous (liquid) phase and $\alpha_P$ for the discontinuous (particulate) phase, are physical constants of the materials. In a dispersed system intrinsic absorption occurs inside the particles and in the continuous phase, therefore

$$\alpha_{\text{int}} \approx (1-\phi)\cdot\alpha_L + \phi\cdot\alpha_P \tag{2}$$

Excess attenuation coefficient is usually defined to be the difference between the total attenuation and the intrinsic absorption in pure (particle-free) liquid phase[4],[7]:

$$\alpha_{\text{exc}} = \alpha - \alpha_L \tag{3}$$

With this definition, the excess attenuation coefficient is shown to be the incremental attenuation caused by the presence of particles in the continuous phase. Combining Formulae (1) to (3), it can be seen that

$$\alpha_{\text{exc}} = \alpha_{\text{vis}} + \alpha_{\text{th}} + \alpha_{\text{sc}} + \phi\cdot(\alpha_P - \alpha_L) \tag{4}$$

The viscoinertial, thermal, and elastic scattering terms depend on particle size, but $\alpha_L$ and $\alpha_P$ do not. Thus the excess attenuation coefficient contains a term that does not depend on size. When working with aqueous dispersions and rigid particles, this term can often be neglected, so that

$$\alpha_{\mathrm{exc}} \approx \alpha_{\mathrm{vis}} + \alpha_{\mathrm{th}} + \alpha_{\mathrm{sc}} \tag{5}$$

However, in some emulsions the ultrasonic absorption in the oily phase can be significant. In that case the definition of excess attenuation coefficient given in Formula (3) can be modified as in Formula (6)

$$\alpha_{\mathrm{exc'}} = \alpha - \alpha_{\mathrm{int}} \tag{6}$$

In this situation Formula (5) is still valid. It should be noted that some authors express attenuation coefficient as a reduced quantity $\tilde{\alpha} = (\alpha / f)$, dividing the absolute attenuation coefficient by the frequency.

## 5.3 Specific attenuation mechanisms

### 5.3.1 Scattering

Ultrasonic scattering is the re-direction of acoustic energy away from the incident beam, so it is elastic (no energy is absorbed). The scattering is a function of frequency and particle size.

### 5.3.2 Thermal losses

Thermal losses are due to temperature gradients generated near the surface of the particle as it is compressed by the acoustic wave. The resulting thermal waves radiate a short distance into the liquid and into the particle. Dissipation of acoustic energy caused by thermal losses is the dominant attenuation effect for soft colloidal particles, including emulsion droplets and latex droplets.

### 5.3.3 Viscoinertial losses

Viscoinertial losses are due to relative motion between the particles and the surrounding fluid. The particles oscillate with the acoustic pressure wave, but their inertia retards the phase of this motion. This effect becomes more pronounced with increasing contrast in density between the particles and the medium. As the liquid flows around the particle, the hydrodynamic drag introduces a frictional loss. Viscoinertial losses dominate the total attenuation for small rigid particles, such as oxides, pigments, and ceramics. An explicit calculation of the attenuation due to viscoinertial loss is given in Annex A for the case of rigid particles that are much smaller than the wavelength of sound in the fluid.

### 5.3.4 Non-monotonic relaxation mechanisms

Whereas according to Reference [14] the intrinsic absorption contains contributions that reflect “translational” molecular motion and the relaxation of both “rotational” and “vibrational” degrees of molecular freedom, non-monotonic relaxation mechanisms should be accounted for separately before the required monotonic attenuation spectrum can be obtained. One approach to the identification and quantification of relaxation effects is found in Reference [11].

## 5.4 Linear models

### 5.4.1 Review

The attenuation of ultrasound in a dispersed system is caused by a variety of mechanisms (see 5.3), the significance of which depends on material properties, particle size and sound frequency. Moreover, for some material systems a linear relationship between sound attenuation and particle concentration can be observed up to concentrations of 20 % by volume or more, while for others such a relationship exists only at low concentrations. This situation has led to a variety of models; two principal approaches can be distinguished.

The first is the scattering theory, which aims at the scattered sound field around a single particle. Based on this the propagation of sound through the dispersed system can be calculated. By assuming independent scattering events and neglecting multiple scattering the attenuation turns out to be linearly dependent on the particle concentration.

The fundamentals of the scattering theory were already presented by Rayleigh, but his approach ignored the energy dissipation by shear waves and thermal waves (viscoinertial and thermal losses). A well-known scattering theory is the ECAH (Epstein-Carhart-Allegra-Hawley) theory, a short introduction to which is given in Annex B. The ECAH theory includes sound scattering as well as the viscoinertial and the thermal losses. It can be applied to homogenous, spherical particles with no limit regarding material properties, particle size or sound frequency.

The second principal approach in modelling is to consider only the attenuation by viscoinertial and thermal losses, which is admissible in the long wavelength limit (where $x << \lambda$ or equivalently $k.a << 1$) only. That restriction facilitates the inclusion of nonlinear concentration effects that are caused by the interaction of shear waves and/or thermal waves. Consequently, most of these theories are beyond the scope of this document. However, linear solutions can be obtained in the limiting case of vanishing particle concentration ($\phi \to 0$). In general, these theories then agree with the ECAH theory (with regard to the modelled attenuation mechanism). Purely linear models are that of Urick[15] for the viscoinertial loss mechanism and that of Isakovich[16] for the thermal loss mechanism, both of which agree with ECAH results[7].

The theoretical models sometimes fail to accurately explain measured attenuation spectra, since they hold true only for homogenous, spherical particles and require the knowledge of several physical parameters of the dispersed system. In such situations semi-empirical approaches may be used that are based on the observation that for spheres we get:

$$\tilde{\alpha}_{vis} = g\left(x^2 f\right)$$

$$\tilde{\alpha}_{th} = g\left(x^2 f\right)$$

and

$$\tilde{\alpha}_{sc} = g(x f),$$

where $g$ is an arbitary function.

The application and derivation of such a semi-empirical model is described in Annex C.

### 5.4.2 Physical parameters

A number of physical properties affect the propagation of ultrasound in suspensions and emulsions; these properties (listed in Table 1) are included in the ECAH model described in Annex B. In most practical applications, many of these parameters are not known, and it is therefore difficult to compare theory with experimental observation directly. Fortunately, approximate models can be employed for many situations (cf. see 5.3.1), which reduces the number of influential parameters. Moreover, some of these parameters only weakly affect the attenuation and, therefore, do not need to be known with high accuracy. Typical material systems are listed in Table 2 together with the material properties that most significantly affect the attenuation.

**Table 1 — Complete set of properties for both particle and medium that affect the ultrasound propagation through a colloidal suspension**

| Dispersion medium | Dispersed particle | Units |
|---|---|---|
| Density | Density | kg •m$^{-3}$ |
| Shear viscosity (microscopic) | Shear viscosity (microscopic) Note 2 and 4 | Pa• s |
|  | Shear Modulus Note 3 and 4 | Pa |
| Sound speed | Sound speed | m • s$^{-1}$ |
| Absorption | Absorption | Np•m$^{-1}$, dB•m$^{-1}$ Note 1 |
| Heat capacity at constant pressure | Heat capacity at constant pressure | J• kg$^{-1}$• K$^{-1}$ |
| Thermal conductivity | Thermal conductivity | W• m$^{-1}$• K$^{-1}$ |
| Thermal expansion | Thermal expansion | K$^{-1}$ |

NOTE 1 The decibel (dB) is commonly used as a unit of attenuation, so absorption is often expressed in units of dB/m or dB/cm.

NOTE 2 Shear viscosity of dispersed particles applies to liquid particles i.e. droplets only.

NOTE 3 Shear Modulus applies only to solid particles.

NOTE 4 Shear modulus μ can be replaced by Shear viscosity $\eta_x$ using the relationship $\mu=-i\omega\eta_s$.

**Table 2 — Material properties that have the most significant effect on ultrasonic attenuation**

| System | Properties of the particle | Properties of the liquid |
|---|---|---|
| Rigid submicron particles | Density | Density, sound speed, shear viscosity |
| Soft submicron particles | Thermal expansion | Thermal expansion |
| Large soft particles | Density, sound speed, elastic constants | Density, sound speed |
| Large rigid particles | Density, sound speed, shape | Density, sound speed |

# 6 Determination of particle size

## 6.1 Introduction

This clause describes procedures for estimating the particle size distribution from an ultrasonic attenuation spectrum.

In general, the observed ultrasonic attenuation spectrum, which forms the data function **α**, is dependent on the particle size distribution and on the particle concentration. In dilute suspensions and emulsions, the sound field interacts with each particle independently. That is, the attenuation of sound is formed by the superposition of individual, uncorrelated events, and the spectrum is a linear function of concentration. In this case a linear theory such as the ECAH model described in Annex B can be applied to determine the particle size distribution.

Within the linear theory, the attenuation of sound is related to a PSD by the following formula:

$$\tilde{\alpha}_{exc}(f_i)=\phi\cdot(\tilde{\alpha}_P(f_i)-\tilde{\alpha}_L(f_i))+\phi\cdot\int k(f_i,x)\cdot q_3(x)dx \qquad (7)$$

where ϕ is the volume concentration of the dispersed phase, $q_3(x)$ the volume weighted density function of the PSD. The function $K(f_i,x)$ is called the kernel function, and it models the physical interactions between ultrasound and the particles.

The inversion problem, i.e. determination of the continuous function $q_3(x)$ from a (discrete) attenuation spectrum, is an ill-posed problem: Any measured discrete attenuation spectrum cannot reveal all details of $q_3(x)$. Moreover, signal noise further reduces the amount of accessible information on $q_3(x)$.

For that reason, the inversion problem has to be modified by restricting the space of possible solutions. Two principal approaches can be distinguished:

a) the approximation of $q_3(x)$ by a given PSD function, where the parameters of this function are determined by a nonlinear regression,

b) the discretisation of the size axis $x$ plus imposing additional constraints on the solution vector $\boldsymbol{q}$ (regularization)

These two approaches are described in 6.2.

NOTE The choice of inversion approach does not depend on the choice of theory used to calculate the attenuation spectrum.

The performance of the algorithms depends on the material system, the measurement instrument as well as on the size distribution. It is further related to the information content of the measured attenuation spectrum, which is determined by the covered frequency range, by the signal noise, to a lower extent by the number of frequencies and primarily by the structure of the kernel functions $k(f_i,x)$ [17].

## 6.2 Inversion approaches used to determine PSD

### 6.2.1 Optimization of a PSD function

In the case of colloidal dispersions, i.e. in the long wavelength regime, the spectra are very smooth, so that very little information appears to be contained in the data. In order to extract the PSD from the attenuation data, a model function can be assumed, effectively reducing the number of free parameters to be fit to the data[9]. A typically used model function is the log normal distribution (see Annex A of Reference [18]):

$$q_3(x)=\frac{1}{sx\sqrt{2\pi}}\exp\left[-\frac{1}{2}\left(\frac{1}{s}\ln\frac{x}{x_{50}}\right)^2\right] \tag{8}$$

where $x_{50}$ is the median size and s is the standard deviation of *ln* ($x$).

The solution of the inversion problem is found by minimizing the error in the fit, $\Delta$, which is defined to be the Euclidean distance between two vectors:

$$\Delta=\left\|\alpha_{\exp}-\alpha_{\mathrm{mod}}\right\|=\left[\sum_{n=1}^{N}\left(\alpha_{\exp n}-\alpha_{\mathrm{mod}\,n}\right)^2\right]^{1/2} \tag{9}$$

In Formula (9), $\boldsymbol{\alpha}_{\exp}$ is the measured spectrum, and the spectrum predicted by the model, $\boldsymbol{\alpha}_{\mathrm{mod}}$, is calculated by Formula (7) using for example viscoinertial loss (see Annex A), ECAH (see Annex B), or some other suitable model. Individual components of these vectors are represented by $\alpha_{\exp_n}$ and $\alpha_{\mathrm{mod}_n}$, respectively, and $N$ is the size of the vectors. The model parameters of the best fitting function can be obtained from an optimization strategy. These are iterative algorithms, the general principal of which is described in Annex D. Care shall be taken to ensure that the optimization strategy does not result in a local minimum of the residual Δ, which can cause a significant error in the estimated PSD. Using the parameter values shown in Annex E, Annex F provides a detailed example of how to determine the PSD by iterative optimization of Formula (9).

### 6.2.2 Regularization

Model functions restrict the solution $q_3(x)$ with regard to the number of modes or the skewness, which might obscure relevant details in the distribution function. As shown in Annex C, it is possible to derive an inversion without model parameters for the estimated PSD[19],[20],[21]. If the information content of

$\boldsymbol{\alpha}$ is sufficient, an alternative approach is to introduce size fractions and to re-write Formula (7) in its discrete form:

$$\boldsymbol{\alpha} = \phi \cdot (\boldsymbol{\alpha}_P - \boldsymbol{\alpha}_L) + \phi \cdot \mathbf{K} \cdot \mathbf{q} \tag{10}$$

where the matrix ***K*** is the discrete representation of the ultrasonic model giving the attenuation as a function of particle size. Solving this formula is an ill-conditioned problem, as the signal noise is extremely magnified. Formal solution can yield results that are physically unacceptable, for example negative size fractions or a discontinuous PSD. To avoid such results one can modify the problem by assuming certain properties of the shape of the distribution function (or the solution vector $\boldsymbol{q}$, respectively). The most popular regularisation is based on the smoothness of the distribution function, which can be quantified via $\boldsymbol{q}^{\mathrm{T}} \cdot \boldsymbol{H} \cdot \boldsymbol{q}$ leading to the modified objective function:

$$\chi^2 = \left\| \boldsymbol{\alpha}_{\exp} - \mathbf{K} \cdot \mathbf{q} \right\|^2 + \delta \cdot \mathbf{q}^T \cdot \mathbf{H} \cdot \mathbf{q} \tag{11}$$

In Formula (11) and (12), $\boldsymbol{H}$ is the identity matrix, $\boldsymbol{K}^{\mathrm{T}}$ is the transpose of matrix $\boldsymbol{K}$, and $\delta$ is a suitable Tikhonov regularization factor[19]. The solution is then obtained from:

$$\mathbf{q} = \mathbf{inv}\left( \mathbf{K}^{\mathrm{T}} \mathbf{K} + \delta^2 \cdot \mathbf{H} \right) \mathbf{K}^{\mathrm{T}} \boldsymbol{\alpha}_{\exp} \tag{12}$$

For small values of the regularisation factor δ the solution $\boldsymbol{q}$ is highly affected by the signal noise showing strong oscillations with large negative values. In contrast, very large regularisation factors yield such smooth solutions, that the characteristic features of the PSD are lost. In order to select an optimal regularisation factor, different strategies can be applied[22],[23],[24],[25].

### 6.3 Limits of application

The typical particle size for ultrasonic analysis ranges from 10 nm to 3 mm, although particles outside this range have also been successfully measured. Measurements can be made with a linear model for concentrations of the dispersed phase ranging from 0,1 % by volume up to 5 % or more by volume, depending on the density contrast between the continuous and the dispersed phases. In the case of emulsions, measurements can be made at much higher concentrations (approaching 50 % by volume).

The application of linear theoretical models requires the knowledge of the relevant model parameters. Users should therefore be aware of possible changes in those parameters, for example, variation of the particle concentration. In particular, processes including a change of the phase (e.g. dissolution) or a change in temperature sometimes defy an analysis with theoretical models. In such a case, users are referred to the world of chemometrics, i.e. to methods for data treatment and statistical modelling (e.g. with neural networks, multiple regression).

## 7 Instrument qualification

### 7.1 Calibration

Ultrasonic spectroscopy systems are based on first principles. Thus, calibration in the strict sense is not required; however, it is still necessary and desirable to confirm the accurate operation of the instrument by a qualification procedure. See ISO 20998-1 for recommendations.

### 7.2 Precision

#### 7.2.1 Reference samples

For testing precision, reference samples with an $x_{90}/x_{10}$ ratio in the range of 1,5 to 10 should be used. It is desirable that reference samples used to determine precision are non-sedimenting and comprising spherical particles with diameters in the range of 0,1 µm to 1 µm. The concentration shall be in the range of 1 % to 5 % by volume.

### 7.2.2 Repeatability

The requirements given in ISO 20998-1 shall be followed. The instrument should be clean, and the liquid used for the background measurement should be virtually free of particles. Execute at least five consecutive measurements with the same dispersed sample aliquot or dispersed single shot samples. Calculate the mean and coefficient of variation (CV) for the $x_{10}$, $x_{50}$, and $x_{90}$. An instrument is considered to meet this document for repeatability if the CV for each of the $x_{10}$, $x_{50}$ and $x_{90}$ is smaller than 10 %. If a larger CV value is obtained, then all potential error sources shall be checked.

### 7.2.3 Reproducibility

Reproducibility tests shall follow the same protocol as repeatability. At least three distinct samples of the same reference material shall be measured, and the mean and CV for the $x_{10}$, $x_{50}$, and $x_{90}$ shall be calculated. A CV larger than that of repeatability could be expected due to differences in sampling or dispersion or between analysts or instruments. The certification for the reference material will contain information about the acceptable error for that material.

## 7.3 Accuracy

### 7.3.1 Qualification procedure

In the qualification step, the accuracy of the total measurement procedure is being examined. It is essential that a written procedure is available that describes sub-sampling, sample dispersion, the ultrasonic measurement, and the calculation of the PSD in full detail. This procedure shall be followed in its entirety and the title and version number reported.

### 7.3.2 Reference samples

Certified reference materials (see Reference [26]) are required in the measurement of accuracy. These materials have a known size distribution with an $x_{90}/x_{10}$ ratio in the range of 1,5 to 10. It is preferred that the median size of the certified reference material will be chosen so that it lies within the size range contemplated for the end-use application. For single shot analysis, the full contents of the container shall be used. If sub-sampling is necessary, this shall be done with due care according to ISO 14488 or another method that has been proven to yield adequate results. If a protocol for sampling, dispersion or measurement is not available, the procedure that is used shall be reported with the final results.

### 7.3.3 Instrument preparation

The advice given in ISO 20998-1 should be followed. The instrument should be clean, and the liquid used for the background measurement should be free of particles.

### 7.3.4 Accuracy test

The written test protocol defined in 7.3.1 shall be followed for the accuracy test, which measures the PSD of the selected reference material. Single shot analysis may be applied. Analysis of sub-samples is permitted if the procedure for sub-sampling is also written and is documented to provide good repeatability. Analysis shall be made on five consecutive sample aliquots, and the average value and CV of the median size shall be calculated.

### 7.3.5 Qualification acceptance criteria

The upper and the lower limit of the uncertainty range of the certified values (expanded uncertainty on a 95 % confidence level) give the interval in which the true size values lie with a high probability.

The qualification test shall be accepted as passing the requirement of this document if the resulting measured particle size distribution achieves both of the following criteria:

a) The reported average value of the median size measured in the qualification test is no smaller than 90 % of the minimum value and no larger than 110 % of the maximum value.

b) The reported CV of the median size does not exceed 10 %.

If a larger deviation is obtained, then all potential error sources should be checked. If it is not possible to meet the qualification criteria of this subclause, then this failure shall be noted on the final PSD report.

If a higher standard of accuracy is required for any reason, then a reference material should be chosen with a narrow confidence interval and a total protocol for sampling, dispersion and measurement should be used that guarantees minimum deviation.

## 8 Reporting of results

The particle size distribution results shall be reported according to ISO 20998-1:2006, Clause 5.

# Annex A
(informative)

# Viscoinertial loss model

Viscoinertial loss (see 5.3.3) can be calculated in the long wavelength limit from Formula (A.1). The form shown in this Annex A is from Reference [5], but it is derived from the explicit analytical solutions of Reference [7] and is mathematically equivalent to results obtained by many authors[15],[27],[28].

$$\alpha_{\mathrm{vis}} = \left(\frac{\phi}{2}\right)\left(\frac{C_d^{\infty}}{c\rho}\right)\frac{(\rho' - \rho)^2}{\left[\left(\rho' + \rho C_i^{\infty}\right)^2 + \left(C_d^{\infty}\right)^2 \omega^{-2}\right]} \tag{A.1}$$

where the dissipative and inertial drag coefficients[5] are given by

$$C_d^{\infty} = \frac{9\eta}{2a^2}(1+Y) \tag{A.2}$$

$$C_i^{\infty} = \tfrac{1}{2}\left(1 + \tfrac{9}{2}Y^{-1}\right) \tag{A.3}$$

with the dimensionless parameter Y defined by

$$Y = a\sqrt{\frac{\omega\rho}{2\eta}} \tag{A.4}$$

In Formulae (A.1) to (A.4),

$\alpha$ = viscous attenuation coefficient

$a$ = particle radius

$c$ = speed of sound in liquid

$\omega$ = angular frequency of ultrasound (i.e. 2π times the frequency)

$\rho, \rho'$ = density of the liquid and particle, respectively

$\eta$ = viscosity of the liquid

$\phi$ = volume concentration of the particle

# Annex B
(informative)

# ECAH theory and limitations

## B.1 Introduction

The Epstein-Carhart-Allegra-Hawley (ECAH) theory is derived from the original work by Epstein and Carhart[6] on sound attenuation in liquid/liquid systems (emulsions). Allegra and Hawley[7] later generalized that theory to include elastic solid particles as well as fluid particles in a liquid suspending medium. This theory is one of many linear scattering theories, each of which has made assumptions about the particle system and how it reacts to sound waves (see Figure B.1).

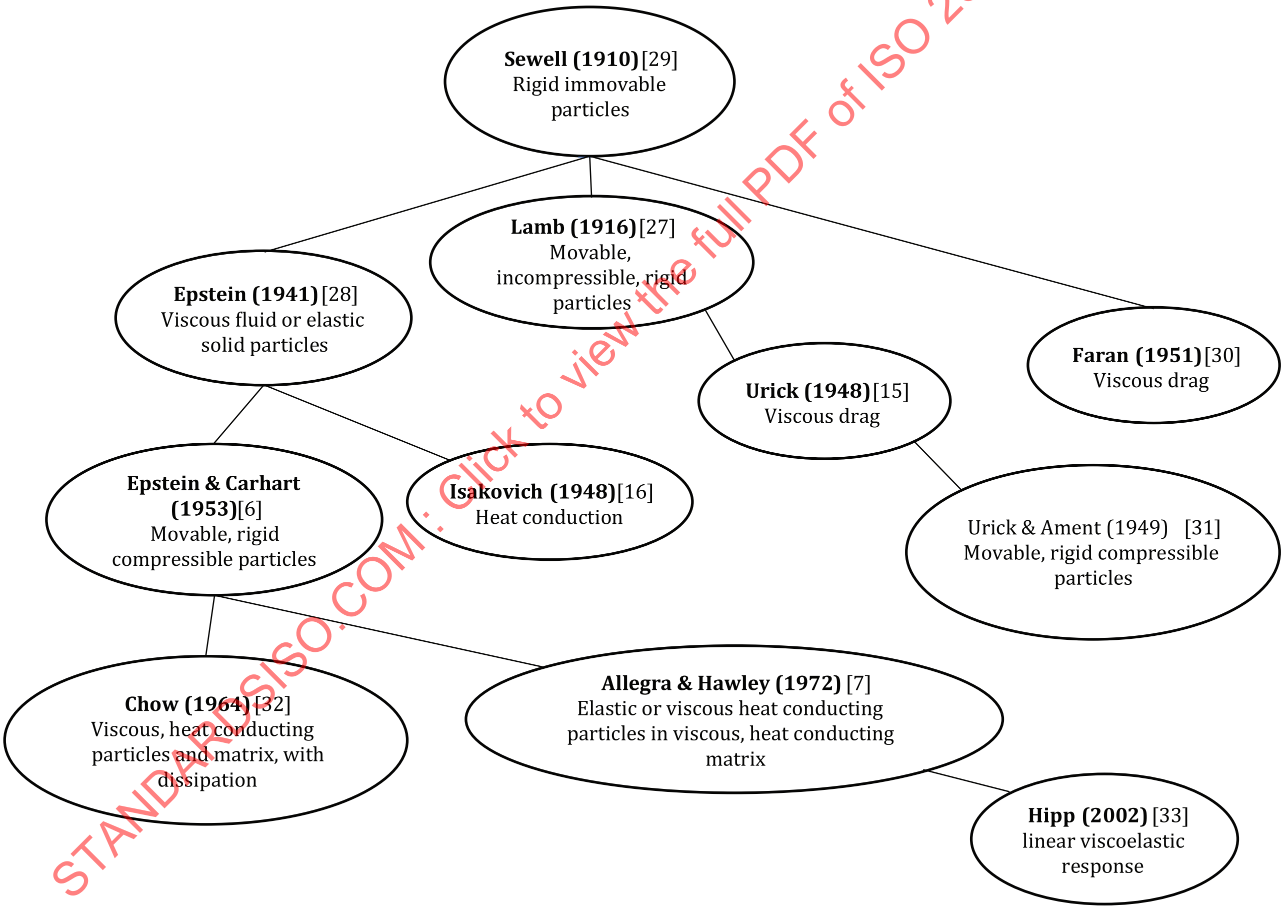

**Figure B.1 — Linear models of ultrasonic scattering**

## B.2 Calculation of attenuation

ECAH theory considers the propagation of sound through a suspension or emulsion via three distinct types of wave: a compression wave $\psi_c$, a thermal wave $\psi_T$, and a shear wave $\psi_s$. Since the incident sound beam is generally a compression wave, the other two types are generated at the boundary of the discontinuous phase. These waves are solutions of the wave equation as given in Formulae (B.1) to (B.3):

$$(\nabla^2 + k_c^2)\psi_c = 0 \tag{B.1}$$

$$(\nabla^2 + k_T^2)\psi_T = 0 \tag{B.2}$$

$$(\nabla^2 + k_s^2)\psi_s = 0 \tag{B.3}$$

The wave numbers $k_c$, $k_T$, and $k_s$ are computed in Formulae (B.4), (B.5), and (B.6):

$$k_c = \frac{\omega}{c} + i\alpha_0 \tag{B.4}$$

$$k_T = (1+i)\sqrt{\frac{\omega\rho C_p}{2\kappa}} \tag{B.5}$$

$$k_s = \sqrt{\frac{\omega^2\rho}{\mu}} \tag{B.6}$$

where $\omega$ is the angular frequency, $c$ is the speed of sound, $\alpha_0$ is the absorption, $\rho$ is density, $C_p$ specific heat at constant pressure, $\kappa$ is the thermal conductivity, $\mu$ is the shear modulus, and $i$ is the imaginary number. These waves appear in the interior of the particle and in the continuous phase (the fluid). Within the fluid, the wave number corresponding to the shear wave (B.6) is calculated by replacing the shear modulus $\mu$ with the factor-$i\omega\eta$, where $\eta$ is the viscosity.

In the case of a spherical particle, the general solution of this system of formulae can be represented as an expansion of Legendre polynomials. The reflected compression wave, for example, is

$$\psi_c^r = \sum_{n=0}^{\infty} i^n (2n+1) A_n h_n(k_c a) P_n(\cos\theta) \tag{B.7}$$

where $h_n$ are Hankel functions of the first kind and $P_n$ are Legendre polynomials. The coefficients $A_n$ specify the reflected compression wave completely. In total, there are six sets of coefficients that describe the three waves in the medium and the three waves inside the particle. These coefficients are related through the boundary conditions, which require continuity of these physical parameters at the surface of the particle: radial velocity, tangential velocity, temperature, heat flux, radial stress, and tangential stress. Explicit formulae for the boundary conditions are given on pages 114 and 115 of Povey[2] for emulsions; the boundary conditions for suspensions of solids are discussed by Allegra and Hawley[7].

The resulting system of formulae is solved to determine the coefficients $A_n$ in Formula (B.7). The ultrasonic attenuation $\alpha$ is then given by[6]

$$\alpha_{\text{exc}} = -\frac{3\phi}{2k_c^2 a^3} \sum_{n=0}^{\infty} (2n+1) \operatorname{Re} A_n \tag{B.8}$$

where $a$ is the radius of the particle.

## B.3 Limitations of ECAH theory

It should be noted that Formula (B.8) is only valid for dilute suspensions, where particle-particle interactions can be neglected.

## B.4 Explicit expressions for simplified ECAH theory including thermal attenuation

In the long wavelength limit, where $k_c a \ll 1$, coefficients of order $n > 1$ can be ignored. This limiting case applies to many suspensions of microscopic particles when the ultrasonic frequency is well below 100 MHz[10]. In this case Formula (B.9) gives,

$$\alpha_{exc} = -\frac{3\phi}{2k_c^2 a^3} \mathrm{Re}\left[A_0 + 3A_1\right] \tag{B.9}$$

Formulae for determining $A_n$ are given by Challis et al.[34] Explicit analytical solutions for $A_0$ and $A_1$ are given by Allegra and Hawley[7] for the long wavelength limit in the case of rigid, dense particles.

The physical meaning of the two coefficients has been discussed by many authors[7],[34]. The $A_0$ term represents the monopole behaviour of the particle and has two components ($A_{01}$ intrinsic loss and $A_{02}$ thermal loss), while $A_1$ represents the dipole behaviour of the particle and is due to viscous loss.

Explicit analytical solutions for $A_0$ (intrinsic and thermal loss) and $A_1$ (viscous loss) are given by McClements[3] and Allegra and Hawley[7]. McClements notes that this approximation is for solid particles but also works well on emulsions. See Formula (B.10).

$$A_0 = \frac{ik^3 r^3}{3}\left[\frac{\rho_1 k_2^2}{\rho_2 k_1^2} - 1\right] - \frac{ik^3 r^3 (\gamma - 1) H}{b_1^2}\left[1 - \frac{\beta_2 \rho_1 C_{p1}}{\beta_1 \rho_2 C_{p2}}\right]^2 \tag{B.10}$$

$$A_1 = \frac{-ik^3 r^3}{9}\left[\frac{[\rho_1 - \rho_2][1 + T + is]}{[\rho_2 + \rho_1 T + i\rho_1 s]}\right]$$

Where

$$s = \frac{9\delta_v}{4r}\left(1 + \frac{\delta_v}{r}\right) T = \frac{1}{2} + \frac{9\delta_v}{4r} \; \frac{1}{H} = \frac{1}{(1 - ib_1)} - \frac{\tau_1}{\tau_2} \cdot \frac{\tan(b_2)}{\tan(b_2) - b_2}$$

$$b_1 = (1+i)\frac{r}{\delta_{t,1}} \; b_2 = (1+i)\frac{r}{\delta_{t,2}} \; \delta_v = \sqrt{\frac{2\eta_1}{\omega\rho_1}} \; \delta_{t,x} = \sqrt{\frac{2\tau_x}{\omega\rho_x C_x}}$$

From Allegra and Hawley, the attenuation of the $A_1$ component can be calculated explicitly

$$\alpha_1 = \frac{\phi \cdot k_1}{2}\left[\frac{[\rho_1 - \rho_2]^2 s}{\left[(\rho_2 + \rho_1 T)^2 + (\rho_1 s)^2\right]}\right] \tag{B.12}$$

Formula (B.12) is identical to the result in Annex A with $C_d^\infty = s\omega\rho$ and $C_d^\infty = s\omega\rho$.

The $A_0$ coefficient can be split into the intrinsic loss $A_{01}$ and the thermal loss $A_{02}$. Determination of intrinsic loss is relatively simple and is given in Formulae (B.13) and (B.14):

$$A_{01} = \frac{-ia_c}{3}\left[a_c^2 - \left(\frac{\rho}{\rho'}\right) a_c'^2\right] \tag{B.13}$$

$$\alpha_{01} = \frac{\phi}{2}\left[\alpha_L\left(-3 + \frac{\rho c^2}{\rho' c'^2}\right) + 2\alpha'_L\left(\frac{\rho c}{\rho' c'}\right)\right] \tag{B.14}$$

However, the determination of thermal loss given in Formulae (B.15) and (B.16) is more difficult due to the complex function *H*:

$$A_{02}=-k_c^2 R_c T_0 \kappa\rho H\left[\left(\frac{\beta}{\rho C_p}\right)-\left(\frac{\beta}{\rho C_p}\right)'\right]^2 \qquad \text{(B.15)}$$

$$\alpha_{02}=\frac{3\phi}{2R^2}cT_0\kappa\rho\left[\left(\frac{\beta}{\rho C_p}\right)-\left(\frac{\beta}{\rho C_p}\right)'\right]^2 \mathrm{Re}(H) \qquad \text{(B.16)}$$

In order to produce a simple solution for the thermal losses, *H* needs to be separated into real and imaginary components, which is not straightforward.

Epstein and Carhart[6] provide a series expansion of the terms and compare the results for different conditions. However, the results are limited. Povey[2] considered the limits of the function and makes an approximation.

Temkin[35] suggests another approach for rigid particles where thermal conduction of the disperse phase is greater than the continuous phase, and uses an approximation given in Formulae (B.17).

$$H=\left[\frac{(1+y_1-iy_1)hy_1{}^2}{i(1+y_1-iy_1(1+hy_1))}\right] \qquad \text{(B.17)}$$

where

$$y=r.\sqrt{\frac{\omega\rho_1 C_{p,1}}{2\tau_1}}$$

and

$$h=\frac{2\rho_2 C_{p2}}{3\rho_1 C_{p1}}$$

which can be separated to provide a real value for *H* as given in Formula (B.18)

$$\mathrm{Re}(H)=\left[\frac{(1+y_1)h^2 y_1{}^3}{(1+y_1)^2+y_1{}^2(1+hy_1)^2}\right] \qquad \text{(B.18)}$$

This result allows a less computationally complex calculation for the thermal attenuation of rigid particles with significant thermal conductivity contrast and emulsions.

# Annex C
(informative)

# Example of a semi-empirical model

There are many semi-empirical models; this annex provides one example.

The ultrasonic extinction $E$ of a suspension or emulsion of mono-disperse particles with the diameter $x$ can be described by the Lambert-Beer's law according to Riebel and Löffler[4].

$$E = -\ln\left(\frac{I}{I_0}\right)_{f_i} = \Delta l \cdot C_{PF} \cdot K(f_i, x) = \alpha \cdot \Delta l$$

The extinction $E$ at a given frequency $f_i$ is linearly dependent on the thickness of the suspension layer $\Delta l$, the projection area-concentration $C_{PF}$ and the extinction efficiency (normalized extinction cross-section).

The extinction efficiency $K$ is a function of frequency and particle size. In a polydisperse system, $K$ is integrated over all particle size fractions from $x_{\min}$ to $x_{\max}$:

$$E(f_i) = \Delta l \cdot C_{PF} \cdot \int_{x_{\min}}^{x_{\max}} K(f_i, x) \cdot q_2(x)\, dx \tag{C.1}$$

The integral in Formula (C.1) can be approximated as a sum:

$$E(f_i) \cong \Delta l \cdot C_{PF} \cdot \sum_j K(f_i, x_j) \cdot q_2(x_j) \cdot \Delta x_j \tag{C.2}$$

If extinction measurements are performed at various frequencies, this results in a linear system of formulae:

$$\begin{pmatrix} E(f_1) \\ \vdots \\ E(f_i) \end{pmatrix} = \Delta l \cdot C_{PF} \cdot \begin{pmatrix} K_{1,1} & \cdots & K_{1,j} \\ \vdots & \ddots & \vdots \\ K_{i,1} & \cdots & K_{i,j} \end{pmatrix} \cdot \begin{pmatrix} q_{21} \cdot \Delta x_1 \\ \vdots \\ q_{2j} \cdot \Delta x_j \end{pmatrix} \tag{C.3}$$

The system of Formulae (C.3) is numerically unstable and must be solved by suitable algorithms.

To calculate the particle size distribution, one must know the extinction cross-section $K$ as the function of the dimensionless size parameter $k.a$ as calculated in Formula (C.4):

$$k.a = \left(\frac{2\pi}{\lambda}\right)\left(\frac{x}{2}\right) \tag{C.4}$$

Figure C.1 shows a typical extinction function for spherical particles.

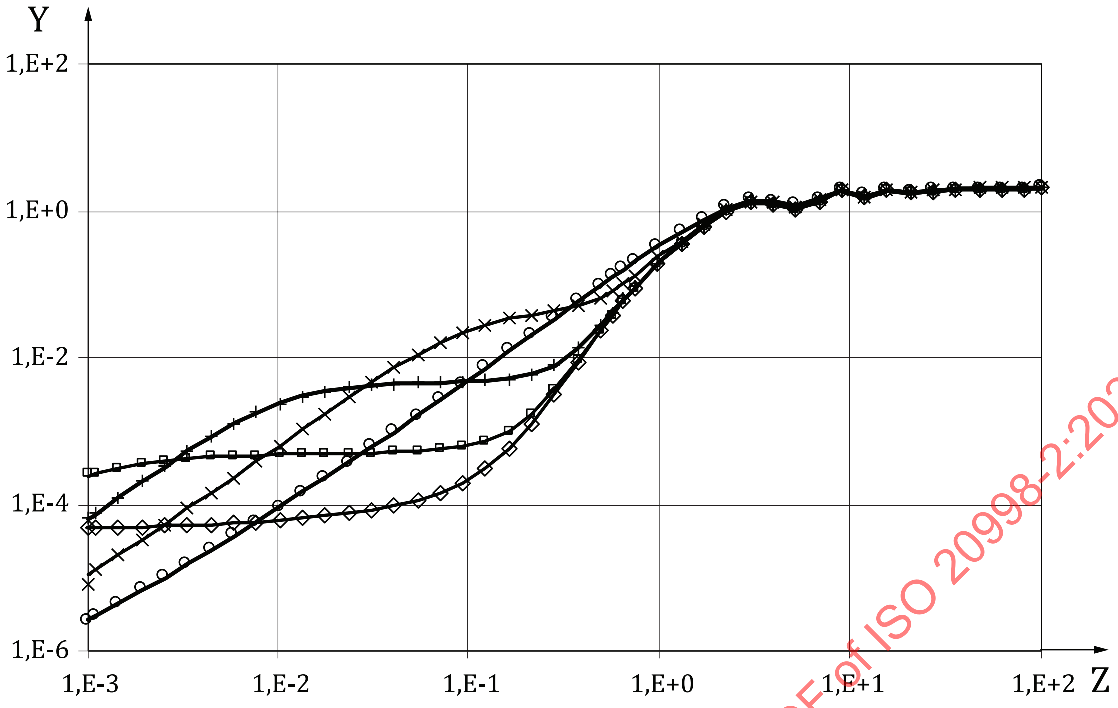

SOURCE: Based on method of Reference [4],

**Key**

| | |
|---|---|
| Y | extinction efficiency K |
| Z | dimensionless size parameter *k.a* |
| ○ | x=0,1 µm |
| × | x=1 µm |
| + | x=10 µm |
| □ | x=100 µm |
| ◇ | x=1 000 µm |

**Figure C.1 — Typical extinction function for spherical glass particles in water**

For small dimensionless size parameters (long wavelength regime) the extinction cross-section can be calculated with ECAH theory. For larger dimensionless size parameters (short wavelength regime) scattering becomes more and more relevant. Particle shape gains a strong influence on the extinction behaviour of the particles. For systems with low density contrast between the continuous and the discontinuous phase, sound absorption within the particle becomes relevant. For many particle systems, the theoretical predictions for the extinction efficiency are not sufficient for the calculation of a particle size distribution.

This situation can be overcome by a semi-empirical approach, which takes advantage of the functional relationship

$$K(f,x)=f(k.a).$$

Firstly, the particle size distribution is measured with a suitable particle sizing method (e.g. laser diffraction), and the frequency dependent ultrasonic extinction is also measured. Secondly, the extinction portion caused by viscous and thermal losses is calculated by a suitable model. The remaining scattering portion of the measured extinction is the starting point for an algorithm which calculates the scattering extinction function with help of the measured particle size distribution. For this, Formula (C.2) is rewritten as Formula (C.5):

$$E(f_i) \cong \Delta l \cdot C_{PF} \cdot \sum_j K\left(f_i, x_j\right) \cdot \Delta Q_2\left(x_j\right) \tag{C.5}$$

where $\Delta Q_2$ is the fraction of a certain particle size class of the total projection area. Formula (C.5) is an ill-posed linear system of formulae, which can be solved according to the methods described in Clause 6. The resulting vector **K** gives the extinction efficiency as a function of the dimensionless size parameter.

The quality of the calculated extinction function depends on the accuracy of the measured particle size distribution. Therefore, the calculation should be carried out with measurements of at least five different samples with different particle size distributions as measured on a well-qualified instrument.

# Annex D
(informative)

# Iterative fitting

Due to the ill-posed nature of the inversion problem, the attenuation spectrum often cannot be inverted directly as in Formula (12) with adequate reliability. Instead, many workers have resorted to an iterative fitting scheme similar to that depicted in Figure D.1. Typically, the spectra are very smooth, so that very little information appears to be contained in the data. In order to extract the PSD from the attenuation data, a model function (such as a log-normal or bi-log-normal distribution) is assumed, effectively reducing the number of free parameters to be fit to the data[9].

a) Measure the attenuation spectrum $\boldsymbol{\alpha}_{\text{exp}}$.

b) Make an initial guess of the PSD, $\boldsymbol{q}$. If a particular shape is assumed for the PSD, this step is equivalent to making an initial guess for the PSD parameters and calculating the PSD. In the case of a log-normal distribution, the parameters are the median size and the geometric standard deviation, and Formula (8) is used to calculate $\boldsymbol{q}$.

c) Assuming that $\phi$ is the particle volume concentration (either known or estimated), the expected attenuation spectrum $\boldsymbol{\alpha}_{\text{mod}}$ is predicted by

$$\boldsymbol{\alpha}_{mod} = \phi \cdot (\boldsymbol{\alpha}_P - \boldsymbol{\alpha}_L) + \phi \cdot \mathbf{K} \cdot \mathbf{q} \qquad \text{(D.1)}$$

where $\boldsymbol{K}$ is a matrix representing the linear model that estimates attenuation as a function of particle size. In cases where the intrinsic attenuation is small, the first term of Formula (D.1) can be omitted.

d) Calculate the error $\Delta$. As given in Formulae (D.2):

$$\Delta = \left[ \sum_{n=1}^{N} \left( \alpha_{\text{exp}_n} - \alpha_{\text{mod}_n} \right)^2 \right]^{1/2} \qquad \text{(D.2)}$$

e) Use an optimization strategy to update the estimate of $\boldsymbol{q}$ (or the parameters used to calculate it) and iterate from step 3 until $\Delta$ becomes sufficiently small. If the concentration $\phi$ is unknown, it may also be varied to decrease the value of $\Delta$. The best results are obtained when the value of $\phi$ is known.

f) The final $\boldsymbol{q}$ is the estimated PSD.

It is understood that simple iterative fitting schemes are prone to find local minima of $\Delta$, so care must be taken to explore an adequately large region of the parameter space. Fitting algorithms are discussed in References [22], [23] and [24].

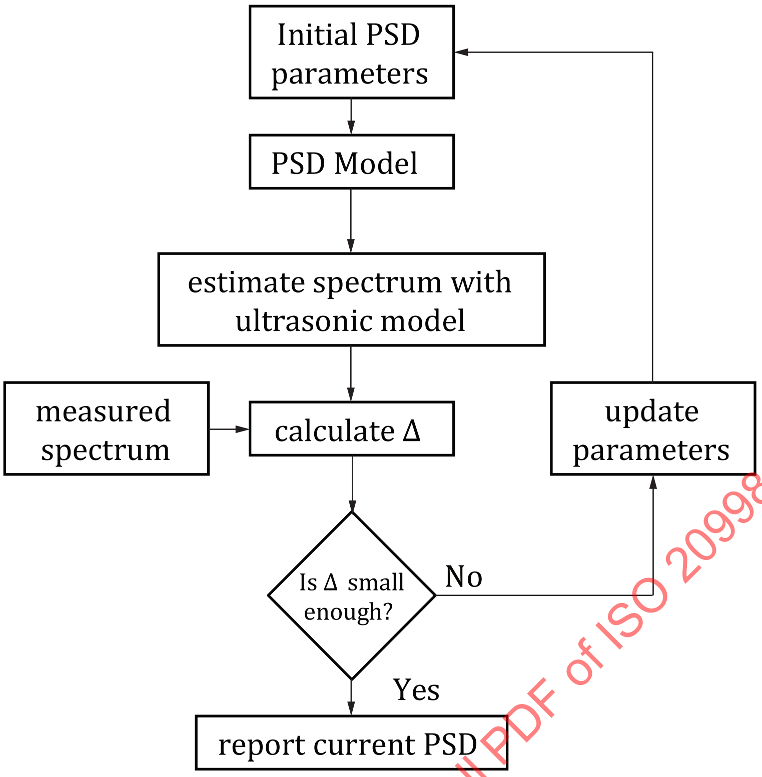

**Figure D.1 — Iterative method of determining the PSD from the measured ultrasonic attenuation spectrum**

# Annex E
(informative)

# Physical parameter values for selected materials

Tables E.1 and E.2 show physical parameter values for a few selected materials; other materials are listed in Reference [10] and [37]. Table E.3 lists examples of standard methods used to measure these parameters.

**Table E.1 — Physical constants for selected solids, as compiled in Reference [10]**

| Parameter | Polystyrene | Silica | TiO2 | Iron |
|---|---|---|---|---|
| $c$ (m·s$^{-1}$) | 2,330 x$10^{3}$ | 5,968 x$10^{3}$ | 7,900 x$10^{3}$ | 5,900 x$10^{3}$ |
| $\rho'$ (kg·m$^{-3}$) | 1,053 x$10^{3}$ | 2,185 x$10^{3}$ | 4,250 x$10^{3}$ | 7,900 x$10^{3}$ |
| $\mu$ (N·m$^{-2}$) | 1,27 x$10^{9}$ | 3,09 x$10^{10}$ | 3,54 x$10^{10}$ | 6,56 x$10^{10}$ |
| $\kappa$ (W·m$^{-1}$K$^{-1}$) | 0,140 | 1,6 | 4,98 | 8,04 x$10^{1}$ |
| $C_{\mathrm{p}}$ (J·kg$^{-1}$K$^{-1}$) | 1,193 x$10^{3}$ | 7,29 x$10^{2}$ | 9,30 x$10^{2}$ | 4,44 x$10^{2}$ |
| $\alpha/f^{2}$ (Np·s$^{2}$m$^{-1}$) | 1,0 x$10^{-13}$ | 2,6 x$10^{-22}$ | 1,2 x$10^{-16}$ | 5,7 x$10^{-14}$ |
| $\beta_{\mathrm{T}}$ (K$^{-1}$) | 2,1 x$10^{-4}$ | 1,35 x$10^{-6}$ | 8,61 x$10^{-6}$ | 3,3 x$10^{-5}$ |

**Table E.2 — Physical constants for selected liquids at 20 °C[37]**

| Parameter | Water (25 °C) | Water (20 °C) | Hexadecane | Isopropanol | Olive oil |
|---|---|---|---|---|---|
| $c$ (m·s$^{-1}$) | 1,487 x$10^{3}$ | 1,483 x$10^{3}$ | 1,358 x$10^{3}$ | 1,181 x$10^{3}$ | 1,440 x$10^{3}$ |
| $\rho$ (kg·m$^{-3}$) | 9,97 x$10^{2}$ | 1,0 x$10^{3}$ | 7,7x$10^{2}$ | 7,9 x$10^{2}$ | 9,00 x$10^{2}$ |
| $\eta$ (Pa·s) | 8,91 x$10^{-4}$ | 1,00 x$10^{-3}$ | 3,10 x$10^{-3}$ | 2,35 x$10^{-3}$ | 8,40 x$10^{-2}$ |
| $\kappa$ (W·m$^{-1}$K$^{-1}$) | 0,59 | 0,59 | 0,14 | 0,13 | 0,19 |
| $C_{\mathrm{p}}$ (J·kg$^{-1}$K$^{-1}$) | 4,182 x$10^{3}$ | 4,182 x$10^{3}$ | 2,090 x$10^{3}$ | 2,494 x$10^{3}$ | 2,00 x$10^{3}$ |
| $\alpha/f^{2}$ (Np·s$^{2}$m$^{-1}$) | 2,5 x$10^{-14}$ | 2,5 x$10^{-14}$ | 1,0 x$10^{-13}$ | 2,7 x$10^{-13}$ | 1,35 x$10^{-12}$ |
| $\beta_{\mathrm{T}}$ (K$^{-1}$) | 2,1 x$10^{-4}$ | 2,1 x$10^{-4}$ | 7,0 x$10^{-4}$ | 1,04 x$10^{-3}$ | 7,2 x$10^{-4}$ |

NOTE Constants for water at 25 °C from Reference [10] are included for comparison in Table E.2.

**Table E.3 — Example standards used to measure parameters listed in Table E.1 and E.2**

| Parameter | Symbol | Standards |
|---|---|---|
| Sound speed | $c$ | ISO 15086-2:2000 |
| Density | $\rho$ | ISO 1183-1:2004, ASTM C128-07a |
| Shear modulus | $\mu$ | ASTM E1875-08 |
| Viscosity | $\eta$ | ISO 3104:1994, ASTM D445 |
| Thermal conductivity | $\kappa$ | ASTM E1952 |
| Specific heat | $C_{\mathrm{p}}$ | ISO 11357-4:2005, ASTM E1269-11 |
| Thermal expansion | $\beta_{\mathrm{T}}$ | ISO 1768:1975 |

NOTE Standards listed in Table E.3 are for information only and it is possible that they do not apply to all materials.

# Annex F
(informative)

# Practical example of PSD measurement

## F.1 Purpose

The purpose of this Annex is to provide one example of how to estimate PSD from an attenuation spectrum using the methods described in this document. This example uses the "Solver" tool in Microsoft Excel to perform the inversion.

NOTE The example given here is for the purpose of demonstration only. Other specimens within the scope of this document can be measured, provided a suitable attenuation model is used in the inversion of the observed attenuation spectra, and other inversion techniques can be used.

## F.2 Attenuation spectrum

The measured attenuation spectrum shown in Figure F.1 is reproduced from an ultrasonic study of various grades of titanium dioxide ($TiO_2$)[9]. The concentration of the $TiO_2$ sample is 1,9 % by volume. Discrete values taken from this curve are shown in Table F.1 for convenience in subsequent calculations.

NOTE Data shown in Figure F.1 and Table F.1 have been extracted from Figure 4 in Reference [9]. The original attenuation data were given in units of Nepers per centimetre; here they are converted into decibels per centimetre.

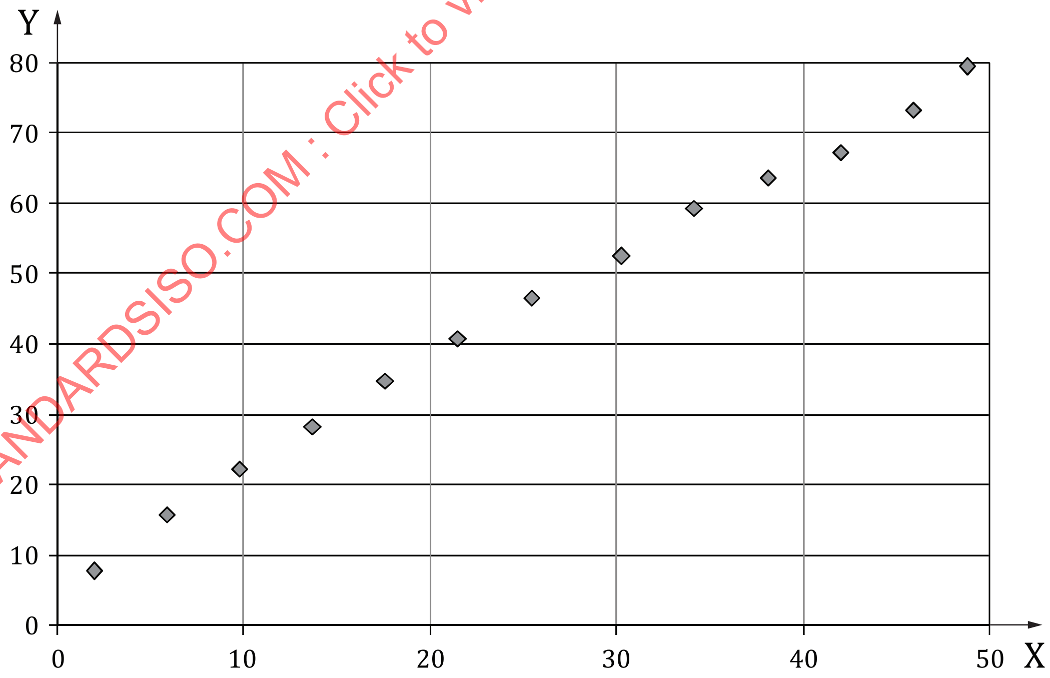

**Key**

X frequency expressed in megahertz

Y attenuation expressed in decibels per centimetre

Figure F.1 — Attenuation spectrum of one $TiO_2$ grade, measured at a concentration of 1,9 % by volume[9]

**Table F.1 — Table of attenuation values depicted in Figure F.1**

| **Frequency**<br>MHz | **Attenuation**<br>dB/cm |
|---|---|
| 1,95 | 7,60 |
| 5,85 | 15,74 |
| 9,76 | 22,25 |
| 13,67 | 28,22 |
| 17,57 | 34,74 |
| 21,48 | 40,71 |
| 25,39 | 46,50 |
| 30,27 | 52,47 |
| 34,17 | 59,35 |
| 38,08 | 63,69 |
| 41,99 | 67,31 |
| 45,89 | 73,28 |
| 48,82 | 79,44 |

## F.3 Choice of model

Titanium dioxide particles are dense (4 250 kg·m$^{-3}$) and fine (<10$^{-6}$ m), so viscous loss is expected to be the dominant attenuation mechanism. The attenuation coefficient is calculated from the viscous loss model shown in Formula (A.1), using the physical parameter values for TiO$_2$ and water (at 25 °C) from[10] as shown in Annex E. The calculation can be implanted as a user-defined function to simplify the spreadsheet. Attenuation is a function of both particle size and frequency; Figure F.2 and Table F.2 show example results of this calculation at three selected values of particle radius.

NOTE 1 The model uses particle radius, but PSD results are generally expressed as particle diameter. This detail must not be overlooked when inverting the attenuation spectrum.

NOTE 2 The calculation shown here is the attenuation per unit volume concentration. This result must be multiplied by the volume fraction $\phi$ (where $0 < \phi < 1$) to obtain the expected attenuation.

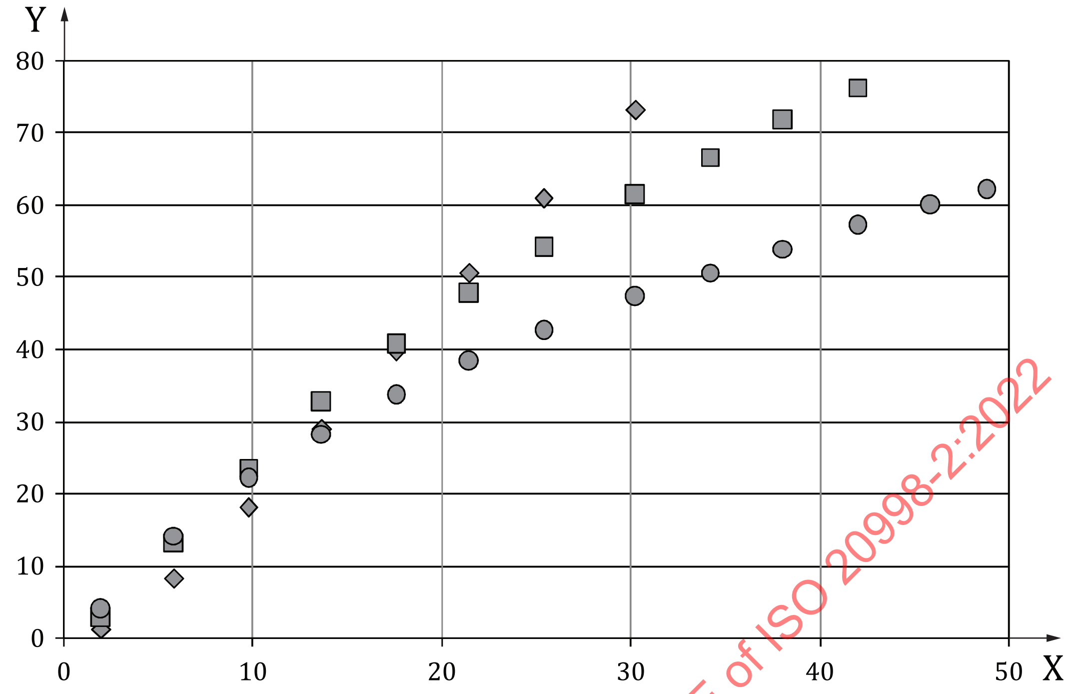

**Key**

X frequency expressed in megahertz

Y attenuation expressed in decibels per centimetre

◆ curve corresponding to particle radius: 8,439 × $10^{-8}$ m

■ curve corresponding to particle radius: 1,458 × $10^{-7}$ m

● curve corresponding to particle radius: 2,100 × $10^{-7}$ m

**Figure F.2 — Viscous-loss model (see A.1) for unit concentration of $TiO_2$**

**Table F.2 — Attenuation coefficient values depicted in Figure F.2**

| **Frequency** MHz | $a$ = 8,439 × $10^{-8}$ m | $a$ = 1,458 × $10^{-7}$ m | $a$ = 2,100 × $10^{-7}$ m |
|---|---|---|---|
| 1,95 | 1,19 | 2,70 | 3,92 |
| 5,85 | 8,12 | 13,19 | 14,07 |
| 9,76 | 17,93 | 23,54 | 21,92 |
| 13,67 | 28,75 | 32,61 | 28,21 |
| 17,57 | 39,68 | 40,53 | 33,51 |
| 21,48 | 50,42 | 47,61 | 38,18 |
| 25,39 | 60,77 | 54,01 | 42,38 |
| 30,27 | 73,07 | 61,26 | 47,12 |
| 34,17 | 82,40 | 66,57 | 50,60 |
| 38,08 | 91,34 | 71,55 | 53,87 |
| 41,99 | 99,88 | 76,25 | 56,96 |
| 45,89 | 108,03 | 80,68 | 59,88 |
| 48,82 | 113,94 | 83,87 | 61,98 |

## F.4 PSD model

Assuming that the volume-weighted PSD can be described as a log-normal distribution[9], then Formula (8) gives the probability that a fraction of the particles' volume lies in the interval $dx$ between $x_0$ and $x_0+dx$[38]. The cumulative PSD, i.e. the volume fraction of particles with diameters between 0 and x, is obtained by integrating Formula (8):

$$Q_3(x)=\int_0^x q_3(x)dx=\left(\frac{1}{s\sqrt{2\pi}}\right)\int_0^x \exp\left[-\frac{1}{2}\left(\frac{1}{s}\ln\frac{x}{x_{50}}\right)^2\right]\frac{dx}{x}=\frac{1}{\sqrt{\pi}}\int_{-\infty}^{z}\exp\left(-z^2\right)dz \tag{F.1}$$

where the substitution variable $z$ is defined by

$$z=\frac{1}{s\sqrt{2}}\ln\left(\frac{x}{x_{50}}\right) \tag{F.2}$$

Since the "error function" is defined by the second integral in (F.1), the cumulative PSD is evaluated as

$$Q_3(x)=\frac{1}{2}+\frac{1}{2}\mathrm{erf}\left[\frac{1}{s\sqrt{2}}\ln\left(\frac{x}{x_{50}}\right)\right] \tag{F.3}$$

Excel has a built-in function, *lognormdist*, which calculates the cumulative log-normal distribution $Q_3(x)$, so it is simple to determine the volume fraction $\phi_n$ in a size class bounded between sizes $x_{n\text{-}1}$ and $x_n$:

$$\phi_n=Q_3(x_n)-Q_3(x_{n-1}) \tag{F.4}$$

NOTE 1 In order to conform to the definitions used here, the correct function call is LOGNORMDIST($x$,LN($x_{50}$),$s$).

NOTE 2 The Geometric Standard Deviation (GSD) of the PSD is equal to exp($s$).

In the example shown in Table F.3, a set of 41 logarithmically-spaced particle diameters is defined in Column A: {$x_1$ = 1,00 × $10^{-8}$ m; $x_2$ = 1,20 × $10^{-8}$ m; $x_3$ = 1,44 × $10^{-8}$ m, ..., $x_{41}$ = 1,47 × $10^{-5}$ m}. These diameters define a set of 40 size intervals (i.e. size classes) where the average particle size $X_n$ of the $n$th class is the geometric mean:

$$X_n=\sqrt{x_{n-1}x_n} \tag{F.5}$$

Using an arbitrary initial guess of $x_{50}$ = 1 × $10^{-7}$ m and $s$ = 0,40, the trial cumulative PSD is calculated in Column B using the *lognormdist* function to evaluate $Q_3(x_n)$ at each particle size. The set of {$\phi_n$} is determined from (F.4) in Column C, and the geometric mean diameter of each size class in Column D is calculated from Formula (F.5).

**Table F.3 — Partial listing of initial entries in an excel spreadsheet**

| | A | B | C | D |
|---|---|---|---|---|
| 1 | x | P(x) | vol fraction | GM diameter |
| 2 | 1,00E-08 | 0,000 0 | | |
| 3 | 1,20E-08 | 0,000 0 | 5,34E-08 | 1,095E-08 |
| 4 | 1,44E-08 | 0,000 0 | 5,76E-07 | 1,315E-08 |
| 5 | 1,73E-08 | 0,000 0 | 5,06E-06 | 1,577E-08 |
| 6 | 2,07E-08 | 0,000 0 | 3,62E-05 | 1,893E-08 |
| 7 | 2,49E-08 | 0,000 3 | 2,11E-04 | 2,272E-08 |
| 8 | 2,99E-08 | 0,001 3 | 1,00E-03 | 2,726E-08 |
| 9 | 3,58E-08 | 0,005 1 | 3,89E-03 | 3,271E-08 |
| 10 | 4,30E-08 | 0,017 4 | 1,23E-02 | 3,925E-08 |